



Assessment of 5G as an ambient signal for outdoor backscattering communications

Ritayan Biswas¹ · Jukka Lempiäinen¹

Accepted: 20 July 2021 / Published online: 4 August 2021
© The Author(s) 2021

Abstract

The aim of this article is to evaluate the applicability of 5G technology as a possible ambient signal for backscattering communications (AmBC). This evaluation considers both urban macro-cellular, small cell as well as rural highway environments. The simulations are performed in outdoor areas including analysis about 5G implementation strategies in different scenarios. Essential aspects of 5G radio network topology such as frequency domain (3.5 GHz and 26 GHz) and antenna locations (offering line-of-sight, LOS) are highlighted and turned to applicability scenarios with AmBC. The LOS scenarios are evaluated to determine the widest applicability area of 5G for AmBC. Typical AmBC applications are studied including collection of data from several sensors to receivers. Evaluation of the applicability of 5G was based on propagation related simulations and calculations utilising the ray tracing technique and the radar equation. The results demonstrate that 5G can be used as an ambient signal for backscattering communications for short ranges for typical sensor sizes. It is also observed that the range of communication is heavily dependent on the the size of the sensor.

Keywords IoT · AmBC · 5G · Sensors

1 Introduction

The internet of things (IoT) is a wireless communication paradigm where sensors are utilised to collect information from the surrounding environment. These sensors may have the capability to measure a multitude of parameters such as temperature, humidity, location, etc. Some of the use cases of these sensors include traffic, atmosphere, health and environment monitoring. Additionally, they have the capability to communicate among themselves and with a central server. Due to the variety of use cases, these sensors will probably be deployed in huge numbers and at a variety of locations. IoT is considered a key enabling technology for future wireless technologies. IoT devices are envisioned to be connected to each other along-with the

internet in order to exchange and transfer different types of data. The fifth generation (5G) of mobile communications is being developed with the provision of supporting the data needs for such a variety of devices.

Ambient backscattering communications (AmBC) is a technology where sensors are capable of harvesting (or, gathering) energy from ambient RF signals present in the atmosphere. AmBC enables battery free and wireless operation of the sensors by harvesting energy from cellular signals, television broadcasts, Wi-Fi signals and so on. Therefore, the requirement for maintenance and changing batteries are eliminated. Thus, AmBC permits the deployment of sensors in some remote as well as inaccessible locations such as inside walls (where certain ambient signals are present). The concept of AmBC was first introduced in [10] during the year 2013. Ambient television broadcast signals were utilised as part of their research and communication distances of 45.7 cm and 76.2 cm were established in indoor and outdoor environments, respectively [10]. Moreover, the channel state information (CSI) and the received signal strength indicator (RSSI) were altered to achieve communication by harvesting ambient Wi-Fi signals [8]. This enabled the sensor type devices to

✉ Ritayan Biswas
ritayan.biswas@tuni.fi

Jukka Lempiäinen
jukka.lempiainen@tuni.fi

¹ Faculty of Information Technology and Communication Sciences, Tampere University (Hervanta Campus), Korkeakoulunkatu 1, Tampere 33720, Finland

be connected to the internet. Data rates of 0.5 kbps and 20 kbps were achieved in the uplink and downlink [8]. There was a significant improvement in throughput achieved in [2] where data rates of 5 Mbps and 1 Mbps were achieved for ranges of 1 m and 5 m, respectively [2].

The AmBC technology can be used for a variety of applications. AmBC works on the principle of radio backscatter, where radio waves generated by a dedicated reader are reflected back from a sensor. Radio backscatter was introduced in literature by Harry Stockman in the year 1948 to identify friendly or hostile air-crafts during the Second World War [17]. The advancement in technology and the reduction in the cost of manufacturing integrated circuits (ICs) has stimulated the development of the radio backscatter technology [19]. This has enabled radio backscatter to become a common and mainstream technology during the past couple of decades [19]. A key application area for radio backscatter is the radio frequency identification (RFID) technology. RFID systems consist of a transmitter, receiver and tag or sensor. The signal generated from the transmitter is reflected back from the sensor. Based on the application scenario, the receiver authenticates the particular sensor. However, these RFID sensors are generally passive elements which are unable to communicate among each other. The communication between passive RFID sensors was introduced in [11] and was achieved by modulating the field of the carrier signal.

Previous studies focused on technologies such as WLAN, FM radio, television broadcasts and existing cellular signals as the possible source of ambient signals for backscattering communications. Presently, the research and development of the fifth generation (5G) of mobile communications is nearly complete (based on Release 15) and the deployment of the system has already taken place in parts of some countries. The 5G system is expected to be widely deployed commercially between 2020 and 2022. The new radio access technology for 5G termed as the 5G new radio (5G NR) was developed by 3GPP and was standardised as the air interface for the 5G systems during the end of 2017. The 5G NR utilises two frequency bands, frequency range 1 (FR1) which utilises the sub 6 GHz microwave frequency band and frequency range 2 (FR2) which utilises the millimeter wave frequency band between 24 GHz and 100 GHz.

The objective of this study is to evaluate the suitability of 5G as an ambient signal for backscattering communications in outdoor environments. The outdoor environment represents the maximum applicability area of 5G for AmBC, due to typical antenna implementations. 5G networks (which support high capacity) are generally deployed in densely populated urban environments (as shown in Fig. 1) at frequencies of 3.5 GHz and 26 GHz. IoT wireless communications are envisioned to have a lot

of use cases in these environments. Therefore, AmBC sensors of different sizes are also studied in order to determine the change in the achievable range of communication due to this parameter. Furthermore, the advent of autonomous vehicles (for example) has led to the research of IoT in rural highway environments. 5G networks can provide coverage to rural highway environment (as shown in Fig. 2). Therefore, the applicability of 5G as an ambient signal for AmBC is also studied in rural highway environment.

2 System setup—5G for Ambient backscattering communications

2.1 Fifth generation (5G) mobile networks

In the near future, mobile communications are envisioned to provide data rates of the order of gigabits and also provide communications with low latency in comparison with present standards. The need for high data rates is driven by the tremendous number of devices that are thought to be connected to the internet and also with the advent of IoT [12]. It is also believed that these data rates would be comparable to fixed-line broadband services. 5G aims to provide support for IoT by enabling more capacity. In IoT wireless communications, a plethora of devices (or, things) are connected to each other as well as a central node via the internet. Additionally, 5G also aims to provide support for technologies such as augmented reality, tactile internet, machine type communications and so on [12]. Furthermore, autonomous vehicles, traffic management and remote surgeries are some of the major use cases behind achieving and establishing ultra reliable low latency communications (URLLC) which is a major requirement of 5G communications [15]. The 5G mobile communications aim to fulfil these requirements by introducing key technologies for the RF interfaces.

Firstly, utilisation of higher frequencies (in comparison with present standards) enable the use of massive multiple-input and multiple-output (MIMO) antenna arrays at the macro-cell base stations [9, 13]. Therefore, the higher path loss resulting from the use of higher frequencies can be compensated by utilising the large antenna arrays at the transmitter. Additionally, advances in the massive MIMO technology and the use of antenna arrays can help in transmission to users distributed along the azimuth and elevation plane simultaneously. Furthermore, beam-forming can help in achieving high performance in both the uplink and downlink [4]. Figure 1 shows the distribution of macro-cell towers in an urban area (for example) where massive MIMO implementation will be carried out.

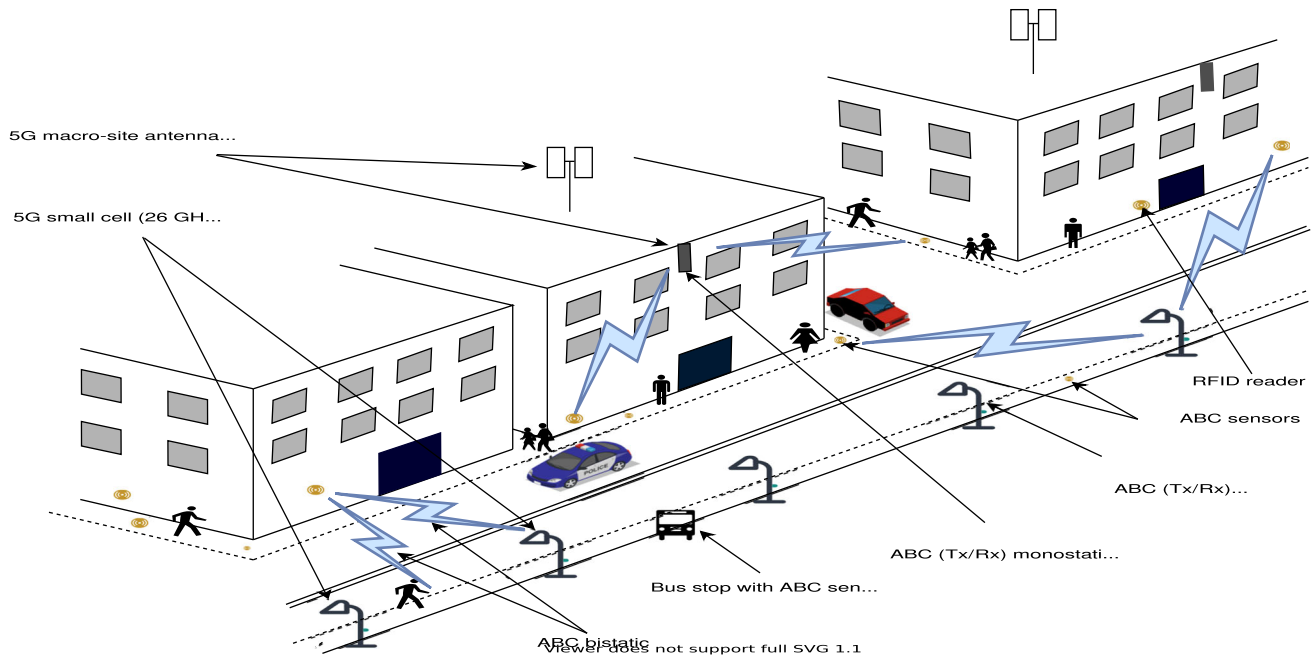


Fig. 1 Deployment strategies of 5G and AmBC in urban environment

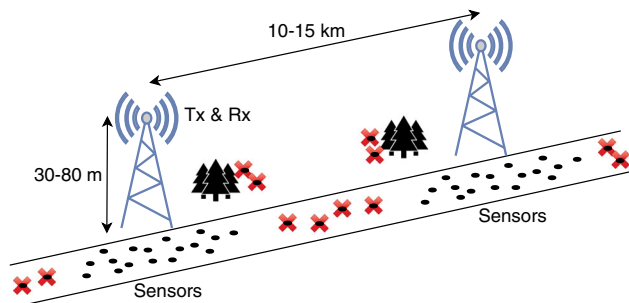


Fig. 2 Rural highway environment

Secondly, the traffic load on dense urban macro-cells can be reduced by utilising small cells in heterogeneous networks. However, to carry the control plane traffic, the requirement and utilisation of macro-cells would still be necessary even if small cells are densely deployed [7]. Figure 1 shows an example of an heterogeneous network environment where small cells are utilised in coherence with traditional macro-cellular networks. Small cells will be implemented for example on top of light-posts located beside the street. The use of heterogeneous networks may result in a higher other cell interference which can affect the capacity gains. However, the excess interference can be compensated by cooperative scheduling and coordinating multipoint (CoMP) technology [7, 16]. Additionally, the 5G air interface and the associated wave-forms need to be defined such that it is flexible enough to support a variety of applications. For 5G new radio (NR) phase 1, 3GPP has decided to utilise OFDM type wave-forms to fulfil these requirements.

Finally, a shift towards higher frequency bands is required in order to support the requirement for very high data rates and enhanced mobile broadband (eMBB) [12]. There is very large carrier bandwidth available in the millimeter wave frequency range (24 GHz–100 GHz) and the utilisation of this bandwidth can help in achieving high data rates. In 5G networks, a combination of the millimeter and the sub-6 GHz microwave frequency bands will be utilised to establish communications. The wide area coverage could be provided by utilising the sub-6 GHz frequency bands in macro-cells. For local and personal area communications, the licensed millimeter wave frequency band could be utilised [6]. The unlicensed frequency bands in the millimeter wave spectrum could be utilised for small cells and short range indoor links [6]. Macro-cells and small cells may operate at different frequencies even for the same operator as shown in Fig. 1. Generally, the 5G macro-cells are mostly implemented on existing sites and small cells are deployed on new sites such as light-posts as shown in Fig. 1.

This study is performed using ambient 5G signals transmitted at frequencies of 3.5 GHz and 26 GHz (utilised in Europe). The 3.5 GHz frequency band is generally utilised on macro sites and has already been deployed in some countries. However, there is also a possibility of utilising the millimeter wave frequency band in macro-cellular environments (as shown in Fig. 1). It is foreseen that small cells will generally operate at the 26 GHz frequency band (in Finland) though the 3.5 GHz frequency band may also be utilised in some cases. As shown in Fig. 1, the

implementation of 5G is carried out in the macro-cell and small cell environments based on the use cases and the number of users that need to be served at a particular location.

2.1.1 Urban macro-cellular

The urban macro-cellular environment has the most number of users both in terms of personal mobile users and “things” which are a key part of IoT wireless communications. Figure 1 shows a schematic diagram of the environment where the 5G urban macro-cellular T_X antenna will be deployed. Generally, the T_X antenna is located on or just below the rooftop level as shown in Fig 1. The antenna is placed below the rooftop to minimise the effect of the back lobe of the antenna radiation pattern. By modifying the base station components and configurations, existing sites can be utilised for the deployment of 5G networks which provides a profitable approach for telecom operators. The height of the T_X antenna in such an environment is typically 20 m–30 m depending on the height of the buildings. The site distance for such environments is approximately 200 m–400 m. There are various line-of-sight (LOS) paths which exist between the T_X antenna and the users because of typical antenna deployments below the rooftop. In this study, we are considering only the scenarios where a LOS path exists between the T_X antenna and the sensors to find out the maximum applicability area of 5G for AmBC.

2.1.2 Small cells

For cellular operators, small cells tend to provide coverage at the cell edge therefore extending the range of communications. Additionally, small cells are also utilised for providing enhancement in network capacity in densely populated urban areas such as city-centers, shopping malls and railway stations. As shown in Fig. 1, small cell T_X antennas may be located on light-posts which helps to provide coverage to a variety of devices. The requirement of small cells is mostly predominant in densely populated areas such as residential areas (as shown in Fig. 1), stadiums and shopping malls. Furthermore, the expansion of coverage to indoor users in dense urban areas is possible due to the use of small cells. These locations have a large number of users both in terms of personal users and devices. Therefore, the requirement for small cells has grown with smart city applications. This study is performed based on the scenarios where a clear LOS path exists between the small cell T_X antenna and the sensor.

2.1.3 Rural highway

This study is also performed in a rural highway environment because obstacles and interference causing signals are at a minimum there. The typical existing site distance in a rural highway environment is between 5 km and 15 km depending on the frequency of operation and height of the T_X antenna towers. Generally, in Finland, the height of the T_X antenna is between 30 m and 80 m. The schematic diagram of a rural highway environment is shown in Fig. 2. The cost effective method for obtaining the best possible coverage is to place the T_X antenna as high as possible. Moreover, due to the lack of obstacles in this environment clear LOS paths exist between the sensors and the T_X antenna. This study analyses the best case scenario which can be achieved in a rural highway environment.

2.2 Ambient backscattering communications (AmBC)

The AmBC technology works on the principle of energy harvesting from ambient RF signals generated from a variety of sources [10]. Enabling the battery free operation of the sensors is a major advantage of AmBC. In addition, as an external power source is not necessary these sensors can be deployed in a variety of locations where regular maintenance is not possible. The three categories which work on the principle of radio backscatter are, mono-static backscatter, bi-static backscatter and ambient backscatter.

A dedicated transmitter/receiver is necessary for the operation of mono-static backscatter systems [3]. In these systems, the transmitted signal is reflected back from the sensor towards the reader for decoding. An example of mono-static backscatter is a traditional RFID system. Automatic authentication systems and contact-less payments are two major applications of RFID systems. In bi-static backscatter, a centrally located carrier emitter transmits the ambient signals [3]. The sensors can be placed around the carrier emitter within a certain distance. The purpose of bi-static systems is different in comparison to mono-static systems as a dedicated reader is not required. Therefore, in comparison with mono-static backscatter, the range of communication for bi-static backscatter systems may be longer in some use cases. However, the transmission of a dedicated signal is still a drawback of the bi-static backscatter systems as is the case with mono-static backscatter systems.

Ambient signals present in the atmosphere are utilised to establish communication in AmBC. The source of the ambient signal can be mobile network, television broadcast, Wi-Fi signal or FM radio to name a few. The communication range of AmBC is dependent on the strength of the ambient RF signals which depends on the frequency of

the transmitted signal. For example, when FM radio signal is utilised as an ambient signal, the achievable communication range is longer than in case where the ambient signal is received from mobile networks due to the lower operating frequency of FM. The sensors utilised for AmBC need to have the necessary hardware to harvest signals from the ambient systems. The operating principle of AmBC is based on the transmission of ‘0’ and ‘1’ from the sensor [10]. The change of state is achieved by changing the antenna impedance states and alternating between the reflecting and the non-reflecting states of the sensor.

The AmBC technology can operate by utilising the principle of mono-static backscatter or bi-static backscatter. In this study, AmBC operates in the mono-static backscatter mode. Fig. 1 demonstrates the 5G implementations where AmBC mono-static backscatter systems are deployed. The T_X antenna of 5G macro-cell or small cell generates the signal which is subsequently reflected back towards the receiver located at approximately the same location. These communication links between the T_X/R_X antenna and the sensor are shown in Fig. 1. Moreover, AmBC can also be utilised for bi-static operation of the sensors. In this case, the ambient signals may come from the 5G T_X antenna, get reflected from a sensor and be received by a user equipment. This scenario is also illustrated in Fig. 1.

3 Simulation setup

Radio propagation simulations are needed in order to evaluate the applicability area of 5G for AmBC. 5G macro-cells and small cell configurations presented in Fig. 1 are analysed based on ray tracing simulations and radar equation calculations. Both ray tracing approach and radar equation are used in order to have a comparison and certain accuracy of the results.

3.1 Ray tracing

The first method used in order to estimate the signal propagation is the ray tracing technique. The principle of the ray tracing technique is based on the signal propagation between two points, the transmitter and the receiver antenna. A detailed and comprehensive description of the propagation environment is required to accurately predict the path the signal travels. A number of parameters such as the size, location and the height of different obstacles such as buildings, trees and light-posts need to be modelled properly to estimate the signal paths correctly. Additionally, the width of the street, building penetration losses, the rooftop and window refraction losses and other parameters need to be defined. Furthermore, diffraction and scattering

losses of the signal also need to be described in detail in order to have a proper design of the simulation environment.

The ray tracing approach utilises the mirror image theory in order to find the exact path the ray travels between the T_X and the R_X antenna. Moreover, this algorithm defines the direction the signal needs to propagate. Eventually, the received signal power is calculated at the R_X antenna. If there is a signal transmitted between two points ‘A’ and ‘B’, the path loss is calculated based on (1) and the loss occurring due to diffraction or reflection is added. Subsequently, as the ray continues till the R_X antenna, the entire path is divided into smaller links.

In the ray tracing method, each individual multi-path signal component is divided into LOS point-to-point links between reflection and diffraction or between T_X and R_X . For example, a transmitted signal may reflect and diffract of three surfaces before it reaches the receiver. Therefore, there would be four LOS links for this particular scenario. The path loss for each LOS link is calculated based on (1) which represents the free space path loss (FSPL) model. Finally, the path loss for each individual LOS link is summed up to obtain the total loss that the signal experiences following that particular path. In (1), the distance (d) between two points of an LOS link is represented in kilometers and the frequency (f) is calculated in megahertz.

$$FSPL = 32.45 + 20 \cdot \log_{10}(d_{\text{km}}) + 20 \cdot \log_{10}(f_{\text{MHz}}). \quad (1)$$

In this study, the sensors are assumed to have a clear LOS connection from both the macro-cell and small cell T_X antennas as shown in Fig. 1. Therefore, there exists only one LOS path between the T_X antenna and the sensors. In other words, the ray tracing technique gets simplified into a single FSPL link. Furthermore, an approximate reflection loss of 20 dB is considered when the signal rebounds from the sensor [14, 18].

3.2 Radar equation

Another method to calculate the range of communication for a T_X/R_X LOS scenario is the radar equation (RE). The radar equation is represented by (2) where the transmitted signal is reflected towards the R_X antenna from the sensor [1]. The range of communication for the radar equation is determined by the sum of the distance between the transmitter and the sensor and the distance between the sensor and the receiver.

$$R = \sqrt[4]{\frac{P_t G_r G_r \lambda^2 \sigma}{(4\pi)^3 P_r L_{\text{add}}}}. \quad (2)$$

There are two types of radar systems, mono-static and bi-static radar. In mono-static radar, the transmitter and the

receiver are located approximately at the same location. Thus, the signal travels via the same path before and after the reflection from the sensor. Therefore, the total range of communication for a mono-static backscatter system is double the distance between the T_X/R_X antenna and the sensor. On the other hand, bi-static radar systems may have a significant separation between the transmitter and the receiver. The transmitted signal gets reflected from the sensor and travels further to reach the receiver for detection. The total range of communication for bi-static radar systems is the sum of the distance between the transmitter and the sensor and the distance between the sensor and the receiver. In this study, a mono-static radar system is considered for calculating the range of AmBC communication utilising 5G ambient signals.

In (2), the range (R) of the radar is calculated for a mono-static system. The range of a bi-static radar system is expressed by dividing the range term (R) into the distance between the transmitter and the sensor (R_t) and the distance between the receiver and the sensor (R_r). All the distances are expressed in meters. The transmit power (P_t), transmitter gain (G_t) and receiver gain (G_r) are specific for a particular system and these values are expressed in the linear scale. In this study, 32 dBi is used for G_t and G_r for all calculations. The radar equation is frequency dependent and λ represents the wavelength of the ambient 5G signal. The size of the sensor (RCS, σ) is expressed in square meters and has a vital role in determining the range of the radar equation. In literature [1], the value of σ signifies a half dipole antenna and is represented by,

$$\sigma = 0.88 \times \lambda^2. \quad (3)$$

The additional loss (L_{add}) accounts for the system and propagation losses which are different from the path loss. For example, obstacles in the the first Fresnel zone in case of LOS communications lead to an additional loss of a few decibels.

3.3 Minimum reception level and path loss

In order to evaluate the total communication distance, the path loss needs to be defined. The calculation of the path loss is done based on the difference between the transmit power (P_t) and the minimum reception level (P_r) of the system. The typical transmit power (P_t) of 40 W (or, 46 dBm) is utilised for the simulations in the urban macro-cell environment [5]. Also, a typical transmit power (P_t) of 4 W (or, 36 dBm) is used for the urban small cell simulations [5]. P_r represents the minimum reception level of the system which generally signifies the limit up to which the received signal is distinguishable from the background noise. The value of P_r is calculated based on (4). The value

of the Boltzmann's constant (k) is $1.38 \times 10^{-23} \text{ J/K}$ and the operating temperature (T) is 290 K.

$$RX_{\text{sensitivity}}(\text{dBm}) = 10 \cdot \log_{10} \left(\frac{kTB}{0.001} \right) + NF + SNR. \quad (4)$$

The carrier bandwidth (B) may vary in 5G as different bandwidths of 50 MHz–400 MHz are supported for example in the 26 GHz frequency band. In order to reduce the effects of the background noise, the large carrier bandwidth can also be split into smaller parts. As an example, the bandwidth values of 1 MHz, 20 MHz and 200 MHz are used for the simulations in this work. The noise figure (NF) and the signal-to-noise ratio (SNR) of the system is considered to be 8 dB and 4 dB, respectively. The values utilised for calculating the minimum reception level is summarised in Table 1.

Utilising the aforementioned values, the receiver sensitivity (P_r) equals -101.97 dBm when the carrier bandwidth is 1 MHz. When a carrier bandwidth of 20 MHz is used P_r is -88.96 dBm and for 200 MHz P_r equals -78.96 dBm. The values of P_r are summarised in Table 2. It can be observed that noise floor increases when carrier bandwidth increases.

The path loss is calculated as a difference of P_t and P_r of the system. It is observed that the path loss is 147.97 dB (1 MHz), 134.96 dB (20 MHz) and 124.96 dB (200 MHz) for macro-cells. For small cells the path loss is 137.97 dB (at 1 MHz), 124.96 dB (20 MHz) and 114.96 dB (200 MHz), respectively. The available path loss decreases once the additional loss (L_{add}) of 10 dB and the reflection loss is considered.

Table 1 Simulation parameters

Parameter	Unit	Value
Transmission power (macrocells, P_t)	dBm	46
Transmission power (smallcells, P_t)	dBm	36
T_X antenna gain (G_t)	dBi	32
R_X antenna gain (G_r)	dBi	32
Boltzmann's constant (k)	J/K	1.38×10^{-23}
Temperature (T)	K	290
Bandwidth (B)	MHz	1, 20, 200
Noise figure (NF)	dB	8
Signal-to-noise ratio (SNR)	dB	4
Additional loss (L_{add})	dB	10
Reflection loss	dB	20

Table 2 Noise floor at different bandwidths (in dBm)

Bandwidth (B)	1 MHz	20 MHz	200 MHz
Noise floor (P_r)	-101.97	-88.96	-78.96

4 Results

In typical 5G urban macro-cellular environments, the network operation is primarily performed utilising the frequency band of 3.5 GHz. Table 3 shows the distances achieved for different carrier bandwidths at 3.5 GHz utilising the ray-tracing technique for the calculations. It is observed that the signal is able to travel 5.37 km from the T_X antenna to the R_X antenna after it is reflected from the sensor (for mono-static communication). This calculation is performed utilising a carrier bandwidth of 1 MHz. A total distance of 1.2 km can be achieved when 20 MHz carrier bandwidth is used. When the carrier bandwidth of 200 MHz is utilised a total distance of 375 m is achievable. It is clearly observed that the increase in the carrier bandwidth decreases the distance. These results indicate distances that can be achieved for mono-static mode of operation.

The radar equation is also utilised in the urban macro-cellular environment to perform simulations in order to determine the achievable range between the T_X and R_X antenna, after reflection from the sensor. Table 4 gives a summary of the achievable distances at 3.5 GHz for different sensor sizes and for different carrier bandwidths. When σ is 0.0004 m^2 (which represents a sensor size of $2 \text{ cm} \times 2 \text{ cm}$), the maximum range of achievable communication is 695 m (at a carrier bandwidth of 1 MHz), 328 m (at 20 MHz) and 184 m (at 200 MHz). This value of σ represents the scenario where the signal has very small surface area to reflect back from. The sensor size of 0.0065 m^2 represents a half-dipole antenna and the maximum range of achievable communication is 1.39 km (at a carrier bandwidth of 1 MHz), 659 m (at 20 MHz) and 370 m (at 200 MHz). The range of achievable communication increases to 1.55 km (at 1 MHz), 734 m (at 20 MHz) and 413 m (at 200 MHz) when the value of σ is 0.01 m^2 (sensor size of $10 \text{ cm} \times 10 \text{ cm}$). As the sensor size is increased to

Table 3 Ray tracing distances (monostatic) at different bandwidths (in meters)

Bandwidth (B)	1 MHz (m)	20 MHz (m)	200 MHz (m)
3.5 GHz	5370	1200	375
26 GHz	225	50	15

Table 4 Distances (in meters) for AmBC with RE at 3.5 GHz frequency with different bandwidths

RCS (σ, m^2)	1 MHz (m)	20 MHz (m)	200 MHz (m)
0.0004	695	328	184
Half-dipole, 0.0065	1394	659	370
0.01	1554	734	413
0.15	3059	1446	813
0.3	3637	1720	967
0.7	4495	2126	1195

0.15 m^2 the total achievable communication range varies between 813 m (at a carrier bandwidth of 200 MHz) and 3.05 km (at 1 MHz). Correspondingly, the achievable communication range is between 967 m–3.63 km when sensor size is 0.3 m^2 and 1.19 km–4.49 km when size of the sensor is 0.7 m^2 . All these distances represent the mono-static mode of operation where the T_X and R_X antenna are co-located. Furthermore, these results are based on LOS connections between T_X/R_X antenna and sensor.

Based on Tables 3 and 4 it can be observed that the achievable range of communication (in mono-static mode of operation) at 3.5 GHz frequency band varies for corresponding carrier bandwidth values for a particular sensor size. For instance, at 200 MHz carrier bandwidth the achievable distance using ray tracing technique (375 m) is similar to the achievable distance using radar equation (370 m) when a half-dipole antenna is utilised as the sensor. However, the achievable range of communication is significantly different for the ray tracing technique (1.2 km) and the radar equation (659 m at the lower carrier bandwidths). The ray tracing technique does not take into account the size of the sensor. Therefore, the corresponding values for a particular sensor size does not match at each carrier bandwidth. Additionally, the results indicate that the ray-tracing technique provides slightly optimistic values in comparison with the radar equation as the calculation is mainly based on plane wave propagation.

It can also be observed that the carrier bandwidth has a significant impact on the achievable range of communication. The increase in the carrier bandwidth decreases the achievable communication distance. For example, the achievable range of communication is three to four times higher when 1 MHz carrier bandwidth is used instead of 200 MHz. Therefore, achievable communication distance is dependent on the type of ambient 5G signal that is transmitted. A 5G pilot signal generally uses narrower carrier bandwidth in comparison with a 5G traffic channel (10 MHz–100 MHz). Furthermore, the height of the building in the macro-cellular environment plays an important role in determining how far away the sensors can

actually be deployed from the T_X antenna. For example, the distance between the T_X antenna and the sensor is $734/2 = 367$ m (at a carrier bandwidth of 20 MHz) when the sensor size is 0.01 m^2 . Therefore, based on the Pythagoras’s theorem, the sensors can be located 365 m away from the building (when the height of the building is 30 m) in the LOS path of the T_X antenna in order to establish communication in mono-static mode of operation.

The accuracy of the results can be analysed based on the varying additional losses (L_{add}) in the AmBC T_X/R_X communication link. Fig. 3 shows the achievable communication range for different carrier bandwidths as a function of the additional loss. In Fig. 3, the additional loss is varied between 0 dB and 20 dB. The additional loss was 10 dB for the calculation of the results in Table 4. It can be observed that when the additional loss decreases, the achievable communication range increases significantly for all the sensor sizes. Therefore, if a certain communication link experiences more loss due to an obstacle, it is still possible to establish communication, although for a shorter range. Therefore, the blocking of the first Fresnel zone due to a larger obstacle (such as a tree or building) can result in greater additional loss which results in shorter achievable distance for communication.

The 5G small cells are expected to operate mostly at 26 GHz frequency band because the required range of communication is generally short. The ray-tracing results corresponding to different carrier bandwidths at 26 GHz

frequency band are summarised in Table 3. From ray tracing calculations, it is observed that the achievable range of communication is 225 m between the T_X antenna and the R_X antenna after the signal is reflected from the sensor (when carrier bandwidth of 1 MHz is utilised). The total achievable distance is 50 m and 15 m when the carrier bandwidth of 20 MHz and 200 MHz are utilised, respectively. The change in achievable communication distance is not impacted due to the height of the T_X/R_X antenna. Additionally, it can be observed from Table 3 that the range of achievable communication decreases heavily when the frequency band is changed from 3.5 GHz to 26 GHz.

The calculation of the total achievable distance is also performed using the radar equation, similar to the urban macro-cellular environment. Table 5 shows a summary of the results at 26 GHz for different carrier bandwidth and different sizes of σ . When σ represents a half-dipole antenna (0.0001 m^2), the achievable range of communication is 105 m (at a carrier bandwidth of 1 MHz), 49 m (at 20 MHz) and 28 m (at 200 MHz). When the value of σ is 0.0004 m^2 ($2 \text{ cm} \times 2 \text{ cm}$), the achievable range of communication is 143 m (at a carrier bandwidth of 1 MHz), 67 m (at 20 MHz) and 38 m (at 200 MHz). When the size of σ increases to 0.01 m^2 which represents a sensor size of $10 \text{ cm} \times 10 \text{ cm}$, the achievable range of communication increases to 320 m (at 1 MHz), 151 m (at 20 MHz) and 85 m (at 200 MHz), respectively. For these three sensor sizes,

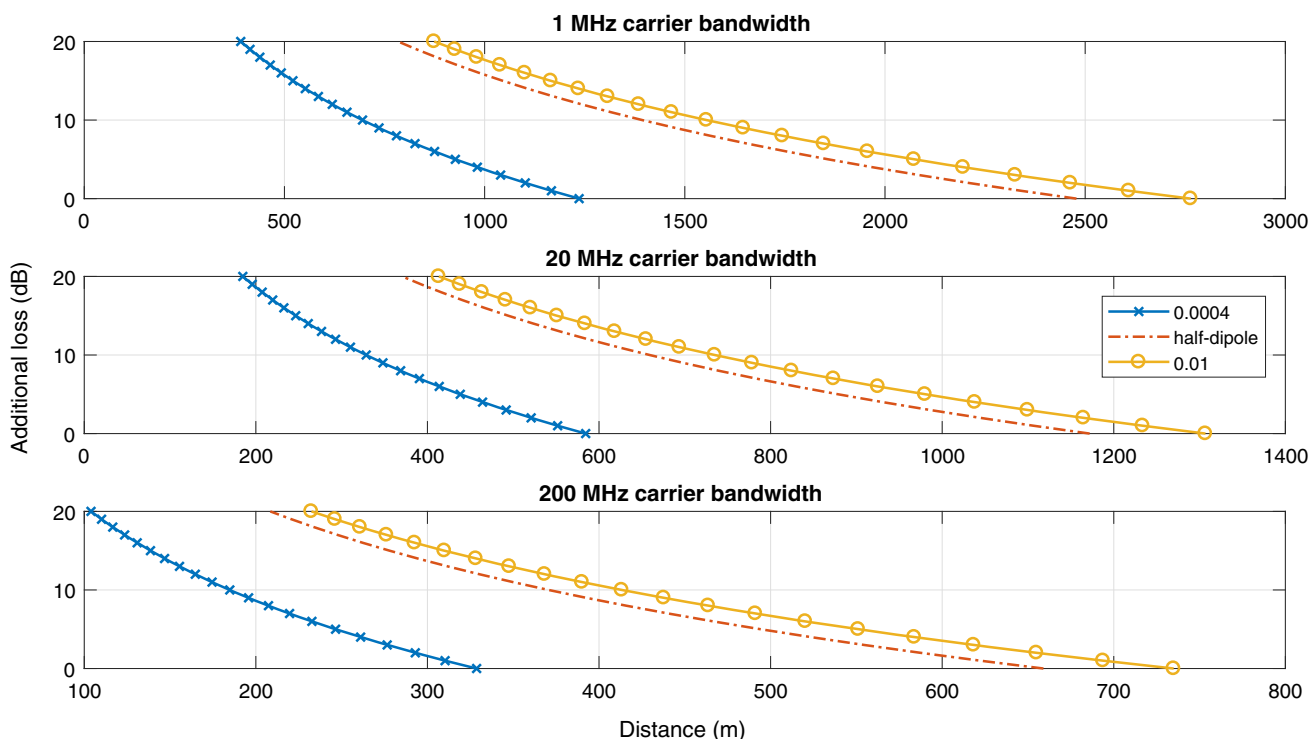


Fig. 3 Achievable distances for different additional losses and carrier bandwidth for varying RCS (σ) at 3.5 GHz

Table 5 Distances (in meters) for AmBC with RE at 26 GHz frequency with different bandwidths

RCS (σ, m^2)	1 MHz (m)	20 MHz (m)	200 MHz (m)
Half-dipole, 0.0001	105	49	28
0.0004	143	67	38
0.01	320	151	85
0.15	631	298	167
0.3	750	354	199
0.7	927	438	246

it can be observed that distances of 28 m–320 m may be possible in mono-static mode of operation depending on the carrier bandwidth utilised. The achievable range of communication is between 167 m–631 m when the size of σ is 0.15 m² and when the carrier bandwidth is varied. When the size of σ is 0.3 m² or 0.7 m², the achievable range of communication varies between 199 m–750 m and 246 m–927 m, respectively. All these results are based on LOS connection between T_X/R_X antenna and the sensor.

Similar to 3.5 GHz frequency band, it is observed that the achievable range of communication for ray tracing and radar equation differs for a particular sensor size when different carrier bandwidths are considered in the calculations. For a half-dipole sensor, the achievable range of communication using the radar equation is 49 m at 20 MHz carrier bandwidth. This is very close to the achievable range of communication using the ray tracing technique (50 m) at the same carrier bandwidth. However, the values at 1 MHz and 200 MHz carrier bandwidth are different for the two techniques. This is due to the ray tracing calculations being independent of the size of the sensor. In this frequency band, the radar equation calculations provide more optimistic values in comparison with the ray-tracing technique.

The range of achievable communication in Table 5 is also heavily dependent on the carrier bandwidth utilised. As the carrier bandwidth is increased, the range of achievable communication decreases. The type of 5G ambient signal also has a major impact on the distance of the communication link. A 5G pilot signal (at 26 GHz) utilises a narrower carrier bandwidth in comparison to a 5G traffic channel (50 MHz–400 MHz). For example, when the size of the sensor is 0.01 m², the range of achievable (mono-static) communication is 85 m at a carrier bandwidth of 200 MHz, which signifies that the sensor can be located at a maximum distance of $85/2 = 42.5$ m from the T_X antenna. However, when a carrier bandwidth of 1 MHz is utilised, the achievable mono-static communication distance is 320 m and the sensor can be located $320/2 = 160$ m from the T_X antenna. One of the 5G small cell base

station deployment scenario is expected to be on top of light-posts which are approximately 10 m in height from the ground. Therefore, the sensors can be served with a signal from the small cell base station as long as they are located in the LOS path and within the proximity of the T_X/R_X antenna.

The accuracy of the results for different additional losses (0 dB–20 dB) are computed and the variation in the achievable range of communication for different sensor sizes is presented in Fig. 4. In Table 5, the calculation of the range of achievable communication was performed using an additional loss of 10 dB. For example, it is observed in Fig. 4 that the communication distance in mono-static mode is 320 m (when the sensor size is 0.01 m²) for an additional loss of 10 dB. However, the achievable range of communication decreases significantly (240 m for an additional loss of 15 dB) as the additional loss increases due to the presence of more obstacles between the T_X/R_X antenna and the sensor. Furthermore, from Fig. 3 it is observed that the achievable range of communication (for a similar sensor size at 3.5 GHz) is 1.55 km (for an additional loss of 10 dB) and decreases to 1.16 km (for an additional loss of 15 dB). It is observed that the mono-static distance for both the frequency bands decreases by approximately 25 percent when the additional loss increases to 15 dB from 10 dB.

In rural highway environments, mono-static communication links can be established with the sensors utilising ambient 5G signals at 3.5 GHz frequency band as long as the achievable range of communication is greater than two times the height of the base station antenna. Distances of 695 m–1.55 km can be achieved for practical sensor sizes of 0.0004 m², half-dipole and 0.01 m², respectively. These communication distances are achieved for sensors located in the LOS path of the T_X antenna. The distance between the sensor and the base station can be calculated using the Pythagoras' theorem. For example, the achievable range of mono-static communication is 695 m (at a carrier bandwidth of 1 MHz) if a sensor of 0.0004 m² is used in the calculations. Therefore, for mono-static mode of operation, the range of achievable communication becomes half ($695/2 = 347$ m) because the signal has to travel back after reflection from the sensor. As illustrated in Fig. 5, when the base station is at a height of 80 m, it is observed that the sensors can be placed 337 m away from it. The achievable range of communication is good for a sensor of size 2 cm \times 2 cm even though the signal is unable to reach near the cell edge. Although the height of the base station antenna has a major impact on the length of the communication link, it is observed that when the height of the base station antenna is reduced to 30 m from 80 m the range of achievable communication does not change significantly. Therefore, in

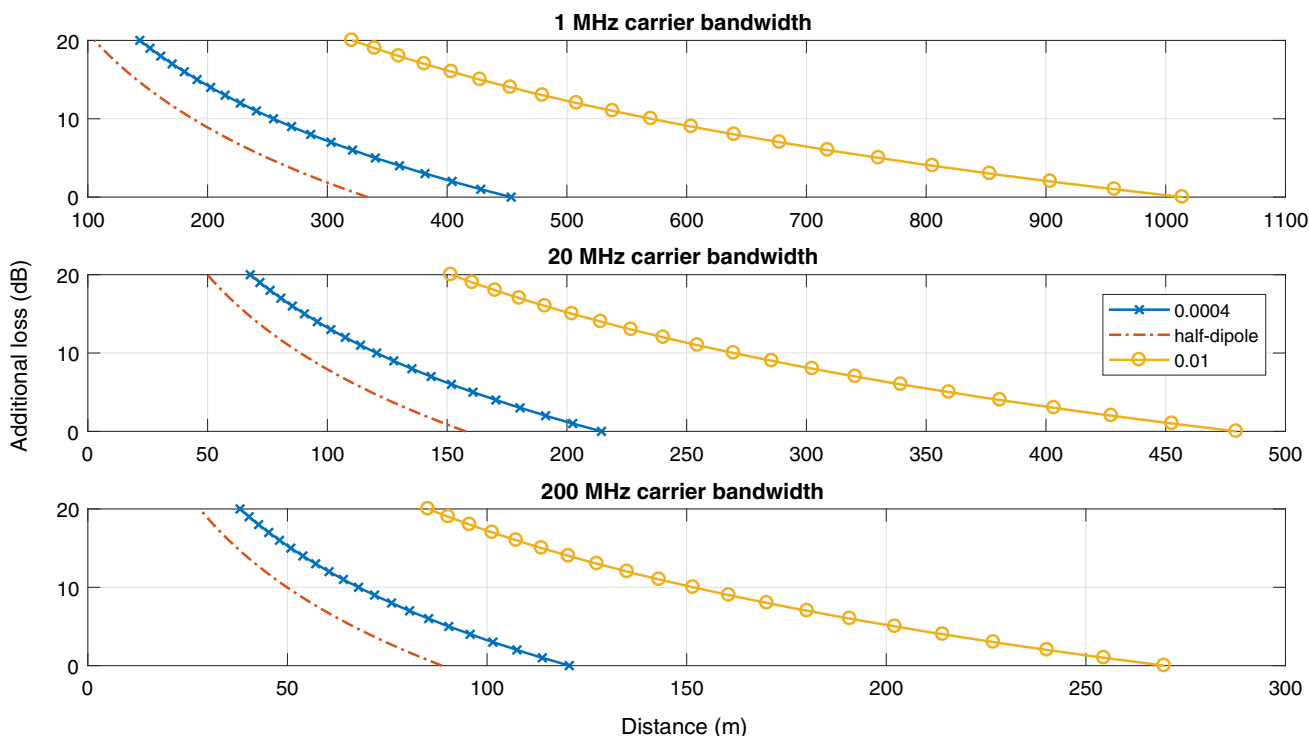


Fig. 4 Achievable distances for different additional losses and carrier bandwidth for varying RCS (σ) at 26 GHz

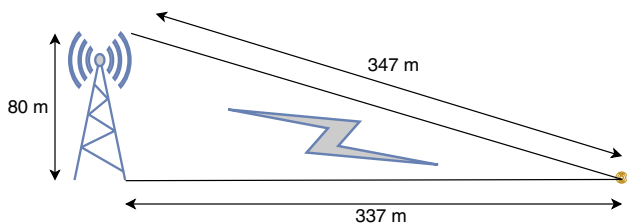


Fig. 5 Illustration of the achievable range of communication in rural highway

order to achieve communication, the sensors need to be located in close proximity of the base station. The additional loss can also be considered to be less than 10 dB as there are generally less obstacles in the rural highway environment. From Fig. 3, it can be observed that for a sensor size of 0.0004 m^2 a total distance of 926 m can be achieved (at 1 MHz carrier bandwidth) between the T_X and the R_X antenna in mono-static mode of operation (when the additional loss is 5 dB). However, in contrast to the 3.5 GHz frequency band, the 26 GHz frequency band is most probably used in a very limited way in the rural 5G environments.

5 Conclusion

The objective of this paper was to evaluate the suitability of 5G as an ambient signal for backscattering communications in the urban macro-cell, small cell and rural environments. The aim was to perform propagation simulations in outdoor environments to analyse different AmBC configurations and geographical areas which can be supported by 5G networks. The AmBC configurations at most typical 5G frequencies of 3.5 GHz and 26 GHz were analysed and it was expected that LOS communication was available between the T_X/R_X antenna and the sensor. In the urban macro-cellular outdoor environment, it was observed that the range of communication at 3.5 GHz was limited to 184 m–4.49 km from the T_X antenna in mono-static mode of operation. In the urban small cell outdoor environment, the 26 GHz frequency band was utilised for the simulations. The sensors located in the LOS path at a distance of 28 m–927 m from the T_X antenna were able to collect information and maintain communication. Additionally, it was observed for both frequency bands that the achievable range of communication significantly changed due to different carrier bandwidth and sensor size. Furthermore, it was observed that the achievable range of communication using the ray-tracing technique did not match with the range achieved utilising the radar equation for a particular sensor size. This was due to the fact the ray-tracing technique did not consider the size of the sensor and the

calculation was based on plane wave propagation. Moreover, it was also observed that the range of communication was heavily dependent on the additional loss (L_{add}) in the communication link. The communication range decreased as the additional loss in the communication link increased. In rural highway environments, sensors located at a distance of 184 m–4.49 km in the LOS of the T_X antenna were able to establish mono-static communication links. Furthermore, based on the results it was observed that the antenna height did not significantly affect the range of communication in rural environments. Therefore, it can be summarised that 5G can be utilised as an ambient signal for AmBC primarily when the sensors are located in the LOS path and in close proximity of the 5G base station T_X antenna.

Acknowledgements The authors would like to thank Tampere University and Academy of Finland for financing the work.

Open Access This article is licensed under a Creative Commons Attribution 4.0 International License, which permits use, sharing, adaptation, distribution and reproduction in any medium or format, as long as you give appropriate credit to the original author(s) and the source, provide a link to the Creative Commons licence, and indicate if changes were made. The images or other third party material in this article are included in the article's Creative Commons licence, unless indicated otherwise in a credit line to the material. If material is not included in the article's Creative Commons licence and your intended use is not permitted by statutory regulation or exceeds the permitted use, you will need to obtain permission directly from the copyright holder. To view a copy of this licence, visit <http://creativecommons.org/licenses/by/4.0/>.

References

- Barton, D., Cook, C., Hamilton, P., & ANRO Engineering, I. (1991). *Radar Evaluation handbook*. Radar Library, Artech House. <https://books.google.fi/books?id=WQJTAAAAMAAJ>
- Bharadia, D., Joshi, K. R., Kotaru, M., & Katti, S. (2015). Backfi: High throughput wifi backscatter. *SIGCOMM Computer Communication Review*, 45(4), 283–296. <https://doi.org/10.1145/2829988.2787490>.
- Choi, S.H., & Kim, D. I. (2015). Backscatter radio communication for wireless powered communication networks. In *2015 21st Asia-Pacific conference on communications (APCC)* (pp. 370–374). <https://doi.org/10.1109/APCC.2015.7412542>
- Ericsson white paper. (2018). *Advanced antenna systems for 5G networks*. <https://www.ericsson.com/en/reports-and-papers/white-papers/advanced-antenna-systems-for-5g-networks>
- European Telecommunications Standards Institute (ETSI). (2020). *Base Station (BS) radio transmission and reception (3GPP TS 38.104 version 15.10.0 Release 15)*
- Hansen, C. J. (2011). Wigig: Multi-gigabit wireless communications in the 60 ghz band. *IEEE Wireless Communications*, 18(6), 6–7.
- Jungnickel, V., Manolakis, K., Zirwas, W., Panzner, B., Braun, V., Lossow, M., et al. (2014). The role of small cells, coordinated multipoint, and massive mimo in 5g. *IEEE Communications Magazine*, 52(5), 44–51.
- Kellogg, B., Parks, A., Gollakota, S., Smith, J. R., & Wetherall, D. (2014). Wi-fi backscatter: Internet connectivity for rf-powered devices. *SIGCOMM Computer Communication Review*, 44(4), 607–618. <https://doi.org/10.1145/2740070.2626319>.
- Larsson, E. G., Edfors, O., Tufvesson, F., & Marzetta, T. L. (2014). Massive mimo for next generation wireless systems. *IEEE Communications Magazine*, 52(2), 186–195.
- Liu, V., Parks, A., Talla, V., Gollakota, S., Wetherall, D., & Smith, J. R. (2013). Ambient backscatter: Wireless communication out of thin air. *SIGCOMM Computer Communication Review*, 43(4), 39–50. <https://doi.org/10.1145/2534169.2486015>.
- Nikitin, P. V., Ramamurthy, S., Martinez, R., Rao, K. V. S. (2012). Passive tag-to-tag communication. In *2012 IEEE international conference on RFID (RFID)* (pp 177–184). <https://doi.org/10.1109/RFID.2012.6193048>
- Osseiran, A., Monserrat, J., Marsch, P., Queseth, O., Tullberg, H., Fallgren, M., Kusume, K., Høglund, A., Droste, H., Silva, I., Rost, P., Boldi, M., Sachs, J., Popovski, P., Gozalvez-Serrano, D., Fertl, P., Li, Z., Sanchez Moya, F., Fodor, G., & Lianghai, J. (2016). *5G Mobile and wireless communications technology*. Cambridge university press. <https://doi.org/10.1017/CBO9781316417744>.
- Rusek, F., Persson, D., Lau, B. K., Larsson, E. G., Marzetta, T. L., Edfors, O., et al. (2012). Scaling up mimo: Opportunities and challenges with very large arrays. *IEEE Signal Processing Magazine*, 30(1), 40–60.
- Samimi, M. K., & Rappaport, T. S. (2014). *Characterization of the 28 ghz millimeter-wave dense urban channel for future 5g mobile cellular*. NYU Wireless TR 1
- Shafi, M., Molisch, A. F., Smith, P. J., Haustein, T., Zhu, P., De Silva, P., et al. (2017). 5g: A tutorial overview of standards, trials, challenges, deployment, and practice. *IEEE Journal on Selected Areas in Communications*, 35(6), 1201–1221.
- Soret, B., Pedersen, K. I., Jørgensen, N. T. K., & Lopez, V. F. (2015). Interference Coordination for Dense Wireless Networks. *IEEE Communications Magazine*, 53(1), 102–109. <https://doi.org/10.1109/MCOM.2015.7010522>
- Stockman, H. (1948). Communication by means of reflected power. *Proceedings of the IRE*, 36(10), 1196–1204. <https://doi.org/10.1109/JRPROC.1948.226245>.
- Wilson, R. M. (2002). *Propagation losses through common building materials 2.4 ghz vs 5 ghz*. Magis Networks, Inc
- Xie, L., Yin, Y., Vasilakos, A. V., & Lu, S. (2014). Managing rfid data: Challenges, opportunities and solutions. *IEEE Communications Surveys Tutorials*, 16(3), 1294–1311. <https://doi.org/10.1109/SURV.2014.022614.00143>.

Publisher's Note Springer Nature remains neutral with regard to jurisdictional claims in published maps and institutional affiliations.



Ritayan Biswas was born in the year 1989 in Kolkata, India. He received his bachelor of technology (B.Tech) degree in Electronics and Communication Engineering from the Institute of Engineering and Management, Kolkata, India in the year 2012. He received his master of science (M.Sc.) degree in Electrical Engineering from Tampere University of Technology, Finland in 2016. Currently, he is pursuing his doctoral studies at Tampere University on future

cellular communications and internet of things (IoT). His general interests include radio network planning and optimization, computer networking and future wireless technologies. He has 5 years of research experience and has authored a few conferences and journal papers and is an IEEE student member.



Jukka Lempiäinen was born in Helsinki, Finland, in 1968. He received an MSc, Lic Tech, Dr. Tech. all in Electrical Engineering, from Helsinki University of Technology, Espoo, Finland, in 1993, 1998, and 1999, respectively. He is a senior partner and the president of European Communications Engineering Ltd. He has altogether more than 10 years of experience in GSM-based mobile network planning and consulting. Currently, he is also

a part-time professor of telecommunications (radio network planning) at Tampere University, Finland. He has written two international books about GSM/GPRS/UMTS cellular radio planning, several international journals, and conference papers, and he has three patents. He is a member of International Union of Radio Science (URSI) national committee, Finland.